Est. 1984

ORIENTAL JOURNAL OF CHEMISTRY
An International Open Access, Peer Reviewed Research Journal

www.orientjchem.org

ISSN: 0970-020 X
CODEN: OJCHEG
2023, Vol. 39, No.(1):
Pg. 189-196

Biosynthesis of CaO Nanoparticles using *Cleome viscosa* Leaf Extract and Investigation of their Antioxidative and Cytotoxicity Activity

HIRDESH SHARMA[1,2], ROMA LAL[3]*, MANEESHA PANDEY[3] and ARCHANA SHRIVASTAV[2]

[1]School of Studies in Micro-Biology, Jiwaji University Gwalior-474009, Madhya Pradesh, India.
[2]College of Life Sciences, Cancer Hospital Campus, Gwalior-474009, Madhya Pradesh, India.
[3]Disciple of Biochemistry, School of Sciences, Indira Gandhi National Open University, New Delhi-110068, India.
*Corresponding author E-mail: lalroma80@gmail.com

http://dx.doi.org/10.13005/ojc/390123

(Received: September 10, 2022; Accepted: January 11, 2023)

ABSTRACT

Cleome viscose Linn. also known as the *jakhya* are widely utilised in traditional and ethnomedicine. Biosynthesis of calcium oxide nanoparticles has captured attention of many as due synthesis involve non-toxic and eco-friendly solvents and ingredients, is more environmentally friendly, least time taking and cost-effective, and simpler than the other alternatives. In the study $CaCO_3$ was obtained from conch shell. CaONPs were biosynthesized in methanolic extract of *Cleome viscosa* leaves through precipitation and deposition of $CaCO_3$. The synthesized CaO nanoparticle was having the average particle size of ~72nm according to DLS and the particle was found to be stable with zeta potential of -21.6mV. The SEM analysis of nanoparticle predicted the structure to be roughly round. The UV-Visible spectrophotometer analysis predicted the maximum absorption in the visible range of ~400-420nm. The synthesized CaO nanoparticle was found to be quite effective against BT-474 breast cancer cell line of conc. 3.4 mg/mL having cell cytotoxicity of ~86% at this concentration and IC_{50} of nanoparticle was 1.359 mg/mL. The IC_{50} of Antioxidative assay was 282 µg/mL and 525 µg/mL for DPPH and ABTS free radicals respectively.

Keywords: *Cleome viscose* leaves, CaO Nanoparticle, Antioxidative activity, Cell Cytotoxicity.

INTRODUCTION

Nanotechnology is a recently evolved discipline that strives to synthesize, modify and apply structures in the nanoscale size of 100nm. These nanoparticles have been widely used in a variety of disciplines of public interest during the last few decades. Nanotechnology has the potential to transform the pharmaceutical sector by providing new tools for molecular illness therapy and quick disease diagnosis. Nanoparticles or nanostructures have higher surface area, large surface potential and distinct surface characteristics[1]. When compared to bulk materials, these nanosized materials have high surface-to-volume ratios. Larger particles' physical properties are stable, have a lower surface

volume ratio, and restrict their use in many areas. Bulk materials display better and unique properties when treated at the nanoscale level due to their size, shape, and morphology[2]. These nanostructures are beneficial in medical, solar energy, and material sciences[3-5]. Calcium oxide (CaO) nanoparticles act as catalyst[6], help in adsorption[7], in purification of water[8], widely used as cosmetic industries[9], in medicines[10], and waste treatment[11]. CaO nanoparticles have been synthesized by several methods like sol-gel[12], gas phase[13], microwave assisted synthesis[8], by chemical precipitation[7] and by electrochemical methods[14].

Green approaches are now mostly used approach to synthesize the nanomaterials. Synthesis by this approach is cost-effective, nontoxic as it does not require use of harmful chemicals, and are environmental favourable. and environmentally friendly[15]. Secondary metabolites, phytochemicals of plant extracts have reducing properties and can reduce a calcium precursor like $CaCl_2$, or $CaCO_3$[16, 11]. CaO is considered to be safe for human beings and environment.

Cleome viscosa (CV) Linn., a type of weed widely distributed in the tropical region of the world including plains of India. The herb is a commonly used remedy for a variety of diseases, according to ethnobotanical research and traditional medicinal systems[17]. *Cleome viscosa* has been studied scientifically against helminths, bacteria, fever, diarrhea, inflammation, liver diseases[18-22].

Therefore, objectives of our study are: 1) to obtain calcium oxide CaONP by the deposition and precipitation of $CaCO_3$ in *Cleome viscosa* leaf extract; 2) to characterize CaO nanoparticles, and 3) to determine the antioxidant activity and its cytotoxicity against MCF-10A (normal) and BT-474 (breast cancer) cell lines.

MATERIAL AND METHODS

Material

Breast cancer cell line BT-474 and MCF-10A were purchased from NCCS, Pune.

Collection of plant sample

Cleome viscose's leaves were collected from the local area in East nimar region (Khandwa) district (21°49'22.08''N, 76°21'8.244''E), Madhya Pradesh in the months of March-April, 2019 and was authenticated by Dr. Anamika, Department of Botany, Vardhman college Bijnor. After cleaning leaves were dried, grounded and stored in dry place. Nearly 200 g of leaf powder was Soxhlet extracted for 3-4 cycles in methanol solvent. Crude extract was dried and weighed. Dried extract was used for further study.

Preparation of $CaCO_3$ from conch shells

The conch shell was ground in a powerful grinder to produce a very fine powder containing nanoparticles of varying sizes. The powder was then sieved in a mechanical sieve, yielding particle sizes ranging from 43 to 150 microns. This powder was kept in a sterile container for further analysis (Figure 2).

Deposition or precipitation of CaO from $CaCO_3$

CaO nanoparticles were prepared following the protocol of Maringgal *et al.,* 2020[23]. In distilled water, a 1M solution of $CaCO_3$ derived from conch shell was prepared. The solution was maintained at room temperature on a magnetic stirrer for 5 h before being filtered. $CaCO_3$ was filtered, dried, and weighed before being mixed in distilled water with an equal amount of *Cleome viscosa* leaf extract to bind with molecules. The mixture was maintained at 60^{0}C overnight followed by two to three days incubation at room temperature. Mixture was diluted in water and filtered overnight followed by thermal deposition at a temperature of ~700^{0}C and was calcinated at 9000 for 1 hour.

Characterization of synthesized CaO nanoparticle

The synthesized CaO nanoparticle was characterized by UV-Vis spectrophotometer, FTIR, DLS Zeta potential and SEM.

UV-Vis spectrophotometer analysis of nanoparticles

The synthesized CaO nanoparticle was scanned from 200 to 800nm. Band gap energy was calculated using tauc plot.

Fourier-Transform Infrared Spectroscopy

Any possible alterations in the functional groups present in the *Cleome viscosa* and CaO nanoparticles were investigated by FTIR spectroscopic measurements using Bruker Optik Alpha-T-FTIR Spectrometer, set in the range of 400-4000 cm^{-1}.

Particle size and distribution

The particle size of synthesized CaO nanoparticle was estimated by dynamic light scattering using Malvern Mastersizer–2000, Canada. Deionized water having refractive index of 1.330 was used as dispersion media. Zeta potential or surface charge of the CaO nanoparticle was estimated after proper dilution. A photon correlation spectrophotometer was used to measure the size distribution of CaO nanoparticles via dynamic light scattering.

SEM analysis

Scanning electron microscopic or SEM analysis was performed using JSM-7610F Schottky Field Emission SEM machine of Japan. The scale and structure of the nanoparticles were covered on the carbon coated copper grid, enabling the grid to be amplified to evaluate the structure and size of the nanoparticles.

Antioxidative activity of CaONP

ABTS assay

ABTS assay was performed according to Pellegrini *et al.,* 1958[24]. Briefly 7mM ABTS in water and 2.45mM potassium persulphate mixed (1:1) incubated in dark for 12-16 hours. The mix is then diluted to get absorbance of ~0.7 at 734nm. Samples were diluted to 1 mg/mL. Samples (Crude, NP) were further diluted in 100, 200, 300, 400 µg/mL concentration and volume make up with ABTS reagent up to 4 mL and incubated in dark for 10 minute. Absorbance were taken at 734nm. Control was prepared by taking absorbance of ABTS and methanol. Standard curve of Ascorbic acid was prepared simultaneously with standards dilution range of 100, 200, 300, 400 µg/mL. ABTS+ scavenging effect (%) was calculated as following equation.

$$\text{ABTS ion scavenging activity } (\%) = \left(\frac{\text{Ab} - \text{Aa}}{\text{Ab}}\right) * 100$$

Ab=Absorbance of reagent control
Aa= Absorbance of sample/standard

IC_{50} of all samples were calculated with their respective standard curve equation.

DPPH assay

DPPH assay was performed using protocol of Blois *et al.,* 1958[25]. Samples were diluted to 1 mg/mL conc. Samples (Crude, NP) were further diluted to 100, 200, 300, 400 µg/mL concentrations and 1 mL 1.0 mL of 0.1 mM of DPPH in methanol was added. Ascorbic acid dilution was prepared in the range of 100, 200, 300, 400 µg/mL. Incubated the reaction mixture for 30 min at RT. Positive control was ascorbic acid. DPPH free radical scavenging activity was calculated as percentage inhibition of free radical and was calculated as follow:

$$\text{DPPH \% inhibiton} = \left(\frac{\text{A0} - \text{At}}{\text{A0}}\right) * 100$$

Where A0 is the absorbance of control (blank without sample) and At is the absorbance of sample. All the tests were performed in triplicate and graph was plotted with mean values.

IC_{50} of all samples were calculated with their respective standard curve equation.

Cytotoxicity assay of CaONP

Cytotoxicity of crude, $CaCO_3$ and CaONPs was estimated by (3-(4,5-Dimethylthiazol-2-yl)-2,5-Diphenyltetrazolium Bromide) assay following the protocol of Mossmann, 1983[26]. The test samples had concentration levels of 1000, 1500, 2000, 2500, 3000, 3500, 4000 and 4500 µg/mL. The diluted samples were mixed together with the cell lines that had been grown for 24 h in a confluent monolayer plate. After 24 h of incubation at 37°C in a 5% CO_2 incubator, the supernatant was collected, and 25 µL of MTT reagent (2 mg/mL) was applied to each well. Following a 2 h incubation period at 37°C, each well received 125 µL of dimethyl sulphoxide to solubilize the formazan precipitate, and the wells were agitated for another 15 minutes. At a wavelength of 490nm, the absorbance was measured using an ELISA reader. Control wells were medium only, DMSO control and Cell control (Well having BT-474 and MCF-10A cells) without the examined chemical.

$$\text{\% Cell cytotoxicity} = \left(\frac{(\text{A0} - \text{A1})}{\text{A0}}\right) * 100$$

Where;

A0 is the absorbance of the Cell control (BT-474, MCF-10A) and A1 is the absorbance of the Cell with crude and CaONPs dilutions.

Cell morphology and cell count (trypan blue dye exclusion assay)

BT-474 cell lines were incubated at the IC_{50} concentrations of the crude, $CaCO_3$ and CaONPs.

Six well microplates were seeded with ~2.6*105 cells/mL. Incubated for 48 hours. in CO_2 incubator with 5% CO_2, 95% air and 99% humidity at 37^{0}C. Cells were visualized under inverted microscope to detect any morphological changes. Cells were then trypsin-zed and centrifuged for pelleting. Pellets were dissolved in 1 mL of DMEM media. Briefly 100-200 µL of the cells were mixed with equal volume of trypan blue (0.4%) and placed on haematocytometer. Observed under the compound microscope in 10X or 40X and counted the coloured (dead) and non-coloured (viable) cells. Counted all the four corners chamber of haematocytometer leaving the middle and below line and calculated the number of cells/ml using the formula:

$$Viable\ count\ (live\ cells/ml) = \left(\frac{number\ of\ live\ cells}{number\ of\ total\ cells}\right) * dilution * 10000$$

Characterization of CaO nanoparticles

CaONPs were synthesised using dried *Cleome viscosa* leaf extract. When dark green methanolic leaf extract was added to $CaCO_3$ followed by thermal deposition, it changed to brownish green, perhaps owing to capping of leaf extract compounds around CaO nanoparticle (Figure 1).

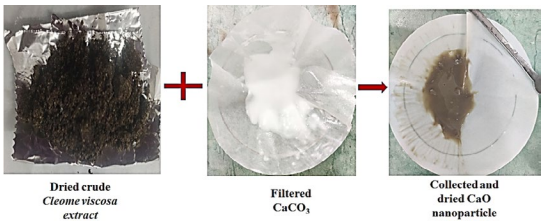

Fig. 1. Biosynthesis of CaONP

C. viscosa leaf extract displayed a maximal absorbance at 206-280nm, according to UV-Visible spectroscopic studies (Fig. 2). The illustration shows that the absorption of CaONPs occurs in the visible area. The UV-Vis of CaONP demonstrates that the nanomaterial has high absorption capability in the visible range[27]. The band gap mapping of CaO nanoparticles was computed approximately 2.673 eV, as shown in Fig. 2C, and the absorption spectra corroborated this. A graph between $(hv)^2$ and hv was used to explore the band gap energy.

$$(\alpha hv) = B(hv - Eg)n$$

Where, B is constant, Eg is band gap energy of CaO and exponent 'n' is the nature of the transition and n=1/2, 2.

The secondary metabolites specially phenols, polyphenolic compounds and flavonoids significantly reduce the Ca ion formation by capping around the nanoparticle[28]. The synthesized CaO nanoparticle through deposition and precipitation is found to have less toxic effect on environment and human due to lack of hazardous chemicals used in chemical synthesis of these nanoparticles[29] and secondary metabolites of extract increases the antioxidative capacity of nanoparticle[30].

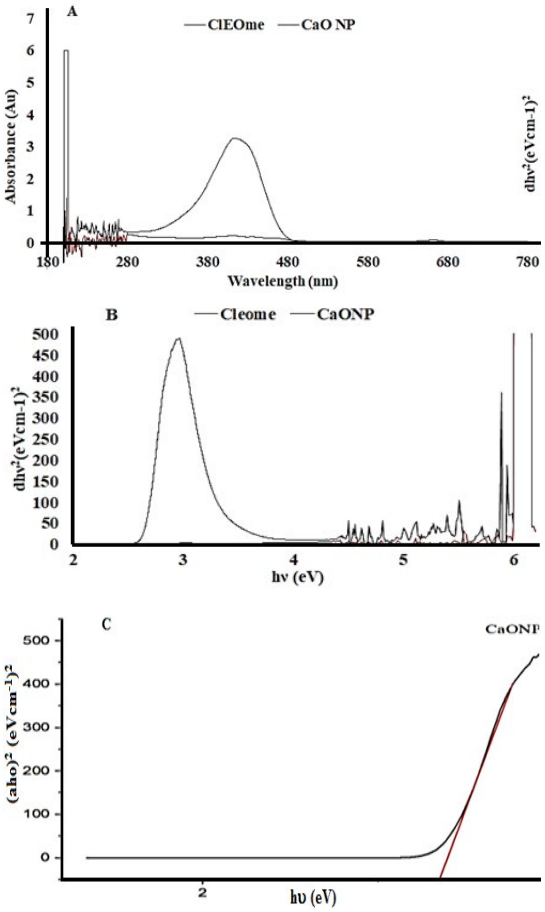

Fig. 2. UV-Visible spectrum and band gap energy analysis: A: UV-Vis spectrum of CaONP and *Cleome viscosa* leaf extract. B: Band gap energy or Tauc plot of CaONP and *Cleome viscosa* leaf extract, C: Tauc plot and estimated band gap energy of synthesized CaONP

Fourier-Transform Infrared Spectroscopy

IR spectroscopy is a strong tool to get an idea on vibrational or rotational levels of a certain molecules. FTIR collects data in a wide range of wavelength and is dependent on the electromagnetic radiation. It describes the many functional groups on the surface of nanoparticles[31].

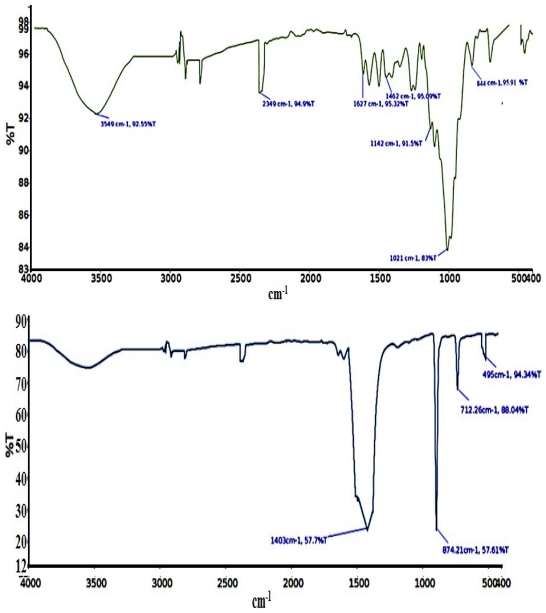

Fig. 3. FTIR spectra of A: *Cleome viscosa* leaf extract, B: CaONP

FTIR spectrum of *Cleome viscosa*, CaO nanoparticle are presented in Fig. 3 to characterize and compare the two. The FTIR result of the *Cleome viscosa* leaf extract showed peaks at 3549, 2349, 1627, 1462, 1142, 1021 and 844 cm^{-1} indicating O-H bond present due water molecule present in leaf extract[32], N-H bond due to presence of amines in extract[33], C=C stretch due to presence of aromatic amines, C-N bends due to presence of amides, C-O bond due to environmental CO_2, C-N or C-O stretch due to aliphatic amines and alcohol, C-Cl stretch due to halides[34] respectively. CaONPs IR spectra revealed key peaks at 1403, 874, 712, and 495 cm^{-1}, with the peak at 1403 cm^{-1} indicating a C-O connection between carbonate and calcium. The existence of a high and sharp peak at 1403 indicates that $CaCO_3$ has not been totally converted to CaO and that there is still a considerable amount of $CaCO_3$. Calcium carbonate's C-O stretching and bending modes feature two well-defined infrared peaks at 1403 and 874 cm^{-1}, respectively[35]. The sharp band at 712 cm^{-1} corresponds to Ca-O bonds, whereas the band at 495 cm^{-1} corresponds to the CaO band[36]. The synthesized CaONP inherited some of the compounds of *Cleome viscosa* leaf extract as indicated from FTIR spectra. There is also a broad peak at 3549 cm^{-1} due to presence of O-H bond and sharp peak of 2349 cm^{-1} due to amines of extract.

Particle size and distribution

Particle size of the synthesized CaONP is found to 72.20nm with an intensity of 88.3% (Fig. 4A). Some minor peaks indicating particle size of 8.91nm was also seen. The results are consistent with SEM findings and near to previous studies of CaONP particle size of 62 nm[37]. The zeta potential of the CaONP was found to be -21.6mV (Fig. 4B) and is in according to earlier reports[37]. The zeta potential analysis indicates the stability of nanoparticle. Negative value of potential indicates its slightly anionic in nature.

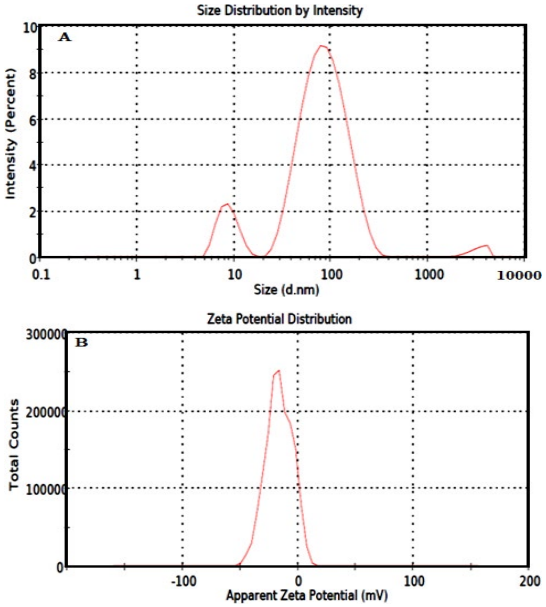

Fig. 4: A: Particle size distribution of synthesized CaONP by intensity, B: Zeta potential of CaONP by DLS

Scanning electron microscopy

SEM images of CaONP was analysed using ImageJ software to estimate the average particle size and morphology of synthesized CaONP. The average particle size estimated by SEM analysis was found to be 75.61nm similar to the findings of particle size distribution. The mean area of the particles is found to be 4183.96nm^2. From the analysis it is revealed that maximum number of particles are in the range of 80 to 90 nm and are in 1000 to 2000nm^2 area. The nanoparticles were found to be irregular in shape (Fig. 5 D). Surface of CaONPs is found to have dents and are not smooth.

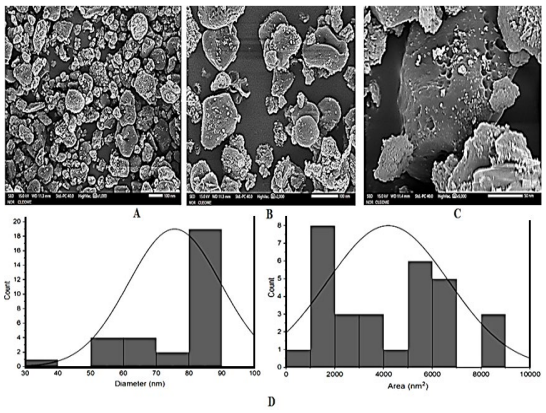

Fig. 5. SEM analysis of CaONP (A,B,C); D: Frequency distribution plot of particle diameter (nm) and Area (nm²) of CaONP

Antioxidative assay

Antioxidant activity and IC_{50} of *Cleome viscosa* and CaONP was estimated by ABTS and DPPH free radicals. The IC_{50} of synthesized CaONP was found to be more effective than the *Cleome viscosa* or $CaCO_3$. IC_{50} for DPPH was estimated to be 533 µg/mL, 502 µg/mL and 283 µg/mL for $CaCO_3$, *Cleome viscosa* extract and CaONP respectively (Fig. 6). While the IC_{50} for ABTS free radicals was found to be 5 mg/mL, 1.06 mg/mL and 525 µg/mL for $CaCO_3$, *Cleome viscosa* extract and CaONP respectively. The CaONP was more effective against DPPH than ABTS free radical.

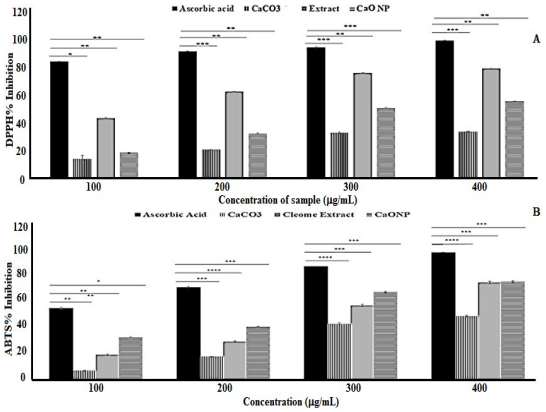

Fig. 6. Antioxidative activity of $CaCO_3$, *Cleome viscosa* leaf extract and CaONP by A: DPPH and B: ABTS assay. Data are mean ± std. dev. Where (n=3)

Cell Cytotoxicity and cell viability assay

Cell cytotoxicity of synthesized CaONP, *Cleome viscosa* crude and $CaCO_3$ was estimated against BT-474 breast cancer cell lines and MCF-10A (control) by MTT assay (Fig. 7). The IC_{50} concentration of CaONPs against BT-474 is found to be ~1.36 mg/mL and that of against MCF-10 is found to be 14 mg/mL. There is not much effect of CaONP on normal cell lines while it can kill ~88.76% of cancer cells at a concentration of 3.5 mg/mL. The IC_{50} of CaONP against lung cancer cell lines (A549) was found to be 92.08 µg/mL[38]. The earlier reported findings and result obtained suggests its applicability against cancer.

The number of viable cells was greatly reduced after an incubation of 48 hours. with IC_{50} concentrations of crude (Fig. 8B) and CaONPs (Fig. 8D) in BT-474 cell lines. While there is no visible decrease in cell viability in $CaCO_3$ treated BT-474 cell lines. Although treatment of the BT-474 cell line with crude and CaONPs inhibited cell proliferation or growth, the number of dead cells as well as the number of viable cells increased in cells treated with $CaCO_3$ (Fig. 8C). There are no morphological changes in the cells, and the cells are properly adhered to the substrate.

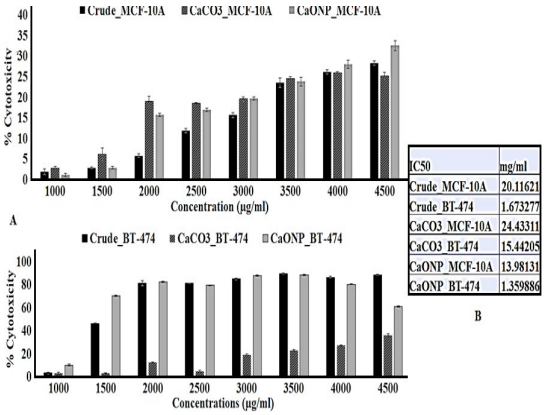

IC50	mg/ml
Crude_MCF-10A	20.11621
Crude_BT-474	1.673277
CaCO3_MCF-10A	24.43311
CaCO3_BT-474	15.44205
CaONP_MCF-10A	13.98131
CaONP_BT-474	1.359886

B

Fig. 7: A: Cell cytotoxicity assay (MTT) against MCF-10A (normal cell line) and BT-474 (breast cancer cell lines), B: 50% inhibitory concentration (µg/mL) of crude, $CaCO_3$ and CaONPs against MCF-10A and BT-474 cell lines. Data are mean±SD. Where n=3

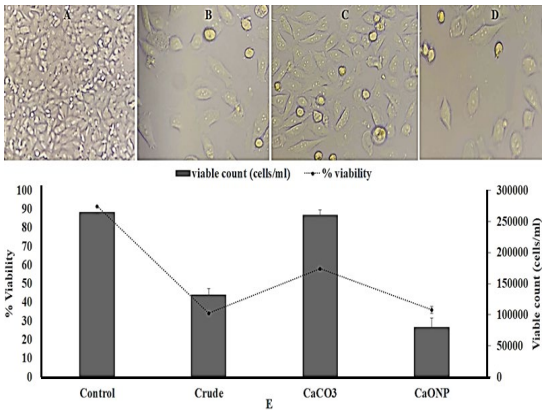

Fig. 8. Cell morphology of BT-474 control (A) and after treatment of IC_{50} concentration of crude (B), $CaCO_3$ (C) and CaONPs after 48 h of incubation. E: Graph showing cell number (cell/mL) after treatment with crude, $CaCO_3$ and CaO nanoparticle along with %viability after 48 hours. of incubations. Data are mean± SD. Where n=3

CONCLUSION

Synthesized CaONP have good anti-oxidative and anticancer activity. The nanoparticle is quite effective against breast cancer cell line. The size of nanoparticle is less than 100nm so it has good capacity to penetrate the cell membrane and diffuse into the cells.

ACKNOWLEDGEMENT

I acknowledge ChemGeneics research foundation, Noida to let me use their lab and facility. I acknowledge Dr. Anamika Singh to help in authenticating the plant. I acknowledge Shraddha Analytical Services, Mumbai for SEM analysis and Lovely professional University for providing Zeta potential and Particle size analysis.

Conflict of interest

The authors state that they have no financial or other conflicts of interest.

REFERENCE

1. Roy, A.; Singh, V.; Sharma, S.; Ali, D.; Azad, A. K.; Kumar, G.; Emran, T. B. *J. Nanomater.*, **2022**, *2022*, 3636481. https://doi.org/10.1155/2022/3636481.
2. Jeevanandam, J.; Barhoum, A.; Chan, Y. S.; Dufresne, A.; Danquah, M. K. *Beilstein J. Nanotechnol.*, **2018**, *9*, 1050–1074. https://doi.org/10.3762/bjnano.9.98.
3. Bashir, R.; Chisti, H. T.; Rangreez, T. A.; Mobin, R. In M. Bhat, I. Wani, & S. Ashraf (Ed.), Applications of Nanomaterials in Agriculture, *Food Science, and Medicine.*, **2021**, 310-329. IGI Global. https://doi.org/10.4018/978-1-7998-5563-7.ch017.
4. Khalfin, S.; Veber, N.; Dror, S.; Shechter, R.; Shaek, S.; Levy, S.; Kauffmann, Y.; Klinger, L.; Rabkin, E.; Bekenstein, Y. *Adv. Funct. Mater.*, **2022**, *32*(15), 2110421. https://doi.org/10.1002/adfm.202110421.
5. Khan, I.; Saeed, K.; Khan, I. *Arabian J. Chem.*, **2019**, *12*(7), 908–931. https://doi.org/10.1016/j.arabjc.2017.05.011.
6. Bankovi–Ili, I. B.; Miladinovi, M. R.; Stamenkovi, O. S.; Veljkovi, V. B. *Renewable Sustainable Energy Rev.*, **2017**, *72*(C), 746–760. https://doi.org/10.1016/j.rser.2017.01.076.
7. Khine, E. E.; Koncz-Horvath, D.; Kristaly, F.; Ferenczi, T.; Karacs, G.; Baumli, P.; Kaptay, G. *J. Nanopart. Res.*, **2022**, *24*, 139. https://doi.org/10.1007/s11051-022-05518-z.
8. Roy A.; Bhattacharya J. *TechConnect Briefs.*, **2011,** *3*, 565–568. https://doi.org/10.1142/S0219581X11008150.
9. Raj, S.; Jose, S.; Sumod, U. S.; Sabitha, M. *J Pharm Bioallied Sci.*, **2012**, *4*(3), 186-193. https://doi.org/10.4103/0975-7406.99016.
10. Butt, A.; Ejaz, S.; Baron, J. C.; Ikram, M.; Ali, S. Dig. *J. Nanomater. Bios.*, **2015**, *10*(3), 799-809.
11. Ferraz, E.; Gamelas, J. A. F.; Coroado, J.; Monteiro, C.; Rocha, F. *Mater. Struc.*, **2018**, *51*(5), 115. https://doi.org/10.1617/s11527-018-1243-7.
12. Habte, L.; Shiferaw, N.; Mulatu, D.; Thenepalli, T.; Chilakala, R.; Ahn, J. W. *Sustainability (Switzerland).,* **2019**, *11*(11), 3196. https://doi.org/10.3390/su11113196.
13. Popok, V.N.; Kylián, O. *Appl. Nano.*, **2020**, *1*(1), 25-58. https://doi.org/10.3390/applnano1010004.
14. Li, N.; Bai, X.; Zhang, S.; Gao, Y. A.; Zheng, L.; Zhang, J.; Ma, H. *J. Dispersion Sci. Technol.*, **2008**, *29*(8), 1059-1061. https://doi.org/10.1080/01932690701815606.
15. Ahmed, S. F.; Mofijur, M.; Rafa, N.; Chowdhury, A. T.; Chowdhury, S.; Nahrin, M.; Islam, A. B. M. S.; Ong, H. C. *Environ. Res.*, **2022**, *204*, 111967. https://doi.org/10.1016/j.envres.2021.111967.
16. Osuntokun, J.; Onwudiwe, D. C.; Ebenso, E. E. *IET Nanobiotechnol.*, **2018**, *12*(7), 888–894. https://doi.org/10.1049/iet-nbt.2017.0277.
17. Senthamilselvi, M.M.; Kesavan, D.; Sulochana, N. *Org. Med. Chem. Lett.*, **2012**, *2*(1),
18. Devi, B. P.; Boominathan, R.; Mandal, S. C. *Phytomedicine.*, **2002**, *9*(8), 739–742. https://doi.org/10.1078/094471102321621368.
19. Mali, R. G.; Mahajan, S.G.; Mehta, A. A. *Pharm. Biol.,* **2007**, *45*(10), 766-768. https://doi.org/10.1080/13880200701585923.
20. Devi, B. P.; Boominathan, R.; Mandal, S. C. *J Ethnopharmacol.*, **2003**, *87*(1), 11–13. https://doi.org/10.1016/s0378-8741(03)00099-0.
21. Gupta, N. K.; Dixit, V. K.; *Indian J Pharmacol.*, **2009**, *41*(1), 36-40. https://doi.org/10.4103/0253-7613.48892.
22. Sudhakar, M.; Rao, Ch. V.; Rao, P. M.; Raju, D. B. *Fitoterapia.*, **2006**, *77*(1), 47–49. https://doi.org/10.1016/j.fitote.2005.08.003.

23. Maringgal, B.; Hashim, N.; Tawakkal, I. S. M. A.; Hamzah, M. H.; Mohamed, M. T. M. *J. Mater. Res. Technol.*, **2020**, *9*(5), 11756–11768. https://doi.org/10.1016/j.jmrt.2020.08.054.
24. Re, R.; Pellegrini, N.; Proteggente, A.; Pannala, A.; Yang, M.; Rice-Evans, C. *Free Radic. Biol. Med.*, **1999**, *26*(9-10), 1231–1237. https://doi.org/10.1016/s0891-5849(98)00315-3.
25. Blois, M.S. *Nat.*, **1958**, *181*, 1199-1200. http://dx.doi.org/10.1038/1811199a0.
26. Mosmann, T. *J. Immunol. Methods.*, **1983**, *65* (1-2), 55-63. https://doi.org/10.1016/0022-1759(83)90303-4.
27. Moghaddas, S. S. T. H.; Moosavi, S. S.; Oskuee, R. K. *Biomass Conv. Bioref.*, **2022**. https://doi.org/10.1007/s13399-022-02643-6.
28. Mohanpuria, P.; Rana, N. K.; Yadav, S. K. *J. Nanopart. Res.*, **2008**, *10*(3), 507-517. https://doi.org/ 10.1007/s11051-007-9275-x.
29. Singh, J.; Dutta, T.; Kim, K.-H.; Rawat, M.; Samddar, P.; Kumar, P. *J. Nanobiotechnol.*, **2018**, *16*(1), 84. https://doi.org/10.1186/s12951-018-0408-4.
30. Filippi, A.; Mattiello, A.; Musetti, R.; Petrussa, E.; Braidot, E.; Marchiol, L. *AIP Conf. Proc.*, **2017**, *1873*(1), 020004. https://doi.org/10.1063/1.4997133.
31. Dutta, A. *Spectroscopic Methods for Nanomaterials Characterization.*, **2017**, *2*, 73–93. https://doi.org/10.1016/B978-0-323-46140-5.00004-2.
32. Mirghiasi, Z.; Bakhtiari, F.; Darezereshki, E.; Esmaeilzadeh, E. *J. Ind. Eng. Chem.*, **2014**, *20*(1), 113–117. https://doi.org/10.1016/j.jiec.2013.04.018.
33. Tizo, M. S.; Blanco, L. A. V.; Cagas AC, Q.; Dela Cruz BR, B.; Encoy, J. C.; Gunting, J. V.; Arazo, R. O.; Mabayo, V. I. F. Sustain. *Environ. Res.*, **2018**, *28*, 326–332. https://doi.org/10.1016/j.serj.2018.09.002.
34. Pillai, L. S.; Bindu, R.; Nair. *J Pharmacogn. Phytochem.*, **2014**, *2*(6), 120-124.
35. Doostmohammadi, A.; Monshi, A.; Salehi, R.; Fathi, M. H.; Golniya, Z.; Daniels, A. U. *Ceram. Int.*, **2011**, *37*(7), 2311-2316. https://doi.org/10.1016/j.ceramint.2011.03.026.
36. Gergely, G.; Weber, F.; Lukacs, I.; Toth, A. L.; Horvath, Z. E.; Mihaly, J.; Balazsi, C. *Ceram. Int.*, **2010**, *36*(2), 803–806. https://doi.org/10.1016/j.ceramint.2009.09.020.
37. Eram, R.; Kumari, P.; Panda, P. K.; Singh, S.; Sarkar, B.; Mallick, M. A.; Verma, S. K. *J. Nanotheranostics.*, **2021**, *2*(1), 51–62. https://doi.org/10.3390/jnt2010004
38. Yoonus, J.; Resmi., R.; Beena, B. *Mater. Today: Proc.*, **2021,** *41*, 535–540. https://doi.org/10.1016/j.matpr.2020.05.246.